Superficies y Vacío ***9****, 271-275, Diciembre 1999*

Structure determination on (Ti,Al)N/Mo multilayers for hard coatings

C.J. Tavares* and L. Rebouta
Departamento de Física, Universidade do Minho, Azurém, 4800 Guimarães, Portugal,

E.J. Alves
ITN, Departamento de Física, E.N.10, 2685 Sacavém, Portugal

(Ti,Al)N/Mo multilayers have been deposited by dc magnetron sputtering on high-speed steel and silicon substrates. Experimental X-ray diffraction (XRD) and computational refinement of these patterns has undergone to achieve the basics to elucidate their structural properties. They were designed with modulation periods of approximately 14 nm, up to a total thickness of 2.8 μm. Residual stress experiments revealed a compressive stress state that prevailed in these structures, ranging from –0.2 to –1.3 GPa. This in turn is in good agreement with the XRD-refined expanded values of the out-of-plane interplanar distances. RBS spectra provided the film composition and a qualitative evolution of the inter-layer roughness with increasing substrate bias potential.

1. Introduction

Multilayers are one-dimensional synthetic structures comprising a number of alternating layers. They are used in a vast range of applications. Wear prevention in steel tools and cutting applications is our major interest to produce (Ti,Al)N/Mo coatings. [1,2]

Both $Ti_{.4}Al_{.6}N$ (fcc) and Mo (bcc) possess a cubic crystal structure and have similar properties, such as: high melting point, good chemical and thermal stability and comparable elastic properties. Since the most interesting and notable properties of multilayers come from combining layers of different materials, it is not surprising that these properties are often strongly sensitive to the nature of the interfaces between them. Therefore, in order to understand the physical behavior of multilayers, it is crucial to determine the detailed structure concealed within the layers and interfaces. Moreover, it is essential to correlate this analysed structure with the measured properties.[3]

2. Fabrication of the samples

(Ti,Al)N/Mo coatings were deposited using a custom made sputtering system. An Ar/N_2 enriched atmosphere was present in the chamber, with an argon flow rate of 140 cm^3/min and a nitrogen flow rate of 8.4 cm^3/min for growing TiAlN, while to produce Mo the Ar flow was varied from 150 to 250 cm^3/min. Pure 200 mm x 100 mm x 6 mm TiAl and Mo targets were used. A current of approximately 0.01 A/cm^2 was applied to both magnetrons. The substrate bias voltage was changed from 0 to -120V while the target-to-substrate distance was kept at 110 mm in all depositions. The base pressure was typically of the order of $5x10^{-5}$ Pa, while the substrate temperature during deposition was 200 ºC. Before deposition the substrates were *in situ* sputter etched in an argon atmosphere of 7 Pa with a dc power of 100 W during 20 minutes.

Two different series of (Ti,Al)N/Mo multilayers were produced with the intention of maintaining in the first (DB series) the modulation periodicity constant, varying the bias voltage and the argon partial pressure at the molybdenum target . In the second series (DC series) a set of thinner multilayers were prepared for RBS measurements. These experimental details are displayed in Table 1.

3. Structural characterization

Rutherford Backscattering Spectrometry (RBS)

Rutherford Backscattering Spectrometry (RBS) technique determined the film composition. A 2 MeV He+ beam in a 3.0 MV Van der Graaf accelerator[4] was used to analyze samples deposited on Si wafers. The backscattered particles were detected by a surface barrier detector placed at 160º with respect to the beam direction in the Cornell geometry and with an energy resolution FWHM of 14 keV. A beam spot of 0.2 mm x 0.6 mm was used. The RBS spectra were fitted with RUMP code.[5]

High-angle XRD and refinement model

For the XRD scans a Philips PW3040/00 X'Pert diffractometer was used in the standard Bragg-Brentano geometry. The specular resolution was 0.002º and the integration time was varied from 1.25 to 5 s with a $2q$ step of 0.01º, for both low-angle and high-angle diffraction experiments.

Knowledge of the crystal texture was derived from XRD at high angles. The multilayer peak positions of the high-angle diffraction spectra are dependent solely of the average lattice spacing on the constituent layers and modulation periodicity.

Structural information regarding the (Ti,Al)N and Mo layers requires the modeling of their superlattice structure. This modeling includes lattice strains, intra- and inter-layer disorder. Thereby, by adjusting the structural parameters of the model to best fit the measured intensities, we determine the structural parameters of the layers. [6,7,8] The SUPREX refinement program was used to fit the experimental high-angle XRD patterns of the (Ti,AN)/Mo multilayers.[6,9] The kinematical step-model[10,11] approach enables the calculation of the average number of atomic planes (N) in an individual layer (TiAlN or Mo) and its associated discrete gaussian width (s_N) and also the atomic interplanar distances in each layer (d_{TiAlN} and d_{Mo}). Additionally, the interfacial width (d_{int}),

*e-mail: ctavares@fisica.uminho.pt

TABLE 1. Experimental details and calculated results regarding the deposition of different series of samples. Bias is the polarization potential applied to the substrate holder and $P^{Mo}(Ar)$ the partial pressure of argon relative to the deposition of Mo. The values of $P^{TiAlN}(N_2)$ were kept constant in all depositions at 0.13 Pa. t_{TiAlN}/t_{Mo} refers to the thickness ratio of the constituent materials in a bilayer of $Ti_{.4}Al_{.6}N$ and Mo, and together with L was obtained from studying the refinements of both the low- and high-angle XRD patterns. The experimental compressive residual stress values and simulated interfacial roughness (s_{Total}) are also shown for the thicker samples.

Sample	Type	P^{TiAlN}(Ar) (Pa)	P^{Mo}(Ar) (Pa)	t_{TiAlN}/t_{Mo}	L (nm)	Bias (V)	Stress (GPa)	s_{Total} (nm)
DB1	$(Ti_{.4}Al_{.6}N/Mo)x200$	0.35	0.6	1.1	13.6	-60	-0.19	0.8
DB 2	$(Ti_{.4}Al_{.6}N/Mo)x200$	0.35	0.6	1.0	13.3	-80	-0.24	0.6
DB 3	$(Ti_{.4}Al_{.6}N/Mo)x200$	0.35	0.6	1.1	13.6	-120	-1.33	-
DB 4	$(Ti_{.4}Al_{.6}N/Mo)x200$	0.35	0.7	1.1	13.5	-60	-0.31	0.8
DB 5	$(Ti_{.4}Al_{.6}N/Mo)x200$	0.35	0.7	1.0	12.8	-80	-0.48	0.7
DB 6	$(Ti_{.4}Al_{.6}N/Mo)x200$	0.35	0.7	1.1	13.6	-120	-1.13	-
DC1	$(Ti_{.4}Al_{.6}N/Mo)x50$	0.35	0.5	1.1	13.6	0	-	-
DC2	$TiAl/(Ti_{.4}Al_{.6}N/Mo)x50$	0.3	0.5	1.1	14.1	-60	-	-
DC3	$Mo/(Ti_{.4}Al_{.6}N/Mo)x50$	0.35	0.7	1.1	12.3	-120	-	-

which varies continuously due to the lattice mismatch between the two materials, and its characteristic gaussian distribution width (s_{int}) can also be determined. The value of the modulation period (Λ) may be calculated from the refined parameters as:

$$\Lambda = (N_{TiAlN} - 1)d_{TiAlN} + (N_{Mo} - 1)d_{Mo} + 2d_{\text{int}} . \qquad (1)$$

Low-angle XRD

In the low-angle regime, the length scales that are probed are greater than the lattice spacing of the constituent layers. Therefore, the scattering solely arises from the chemical modulation of the structure. In low-angle spectra, the modulation period can be assessed through the position of the Bragg diffraction peaks:[12]

$$n = \frac{2\Lambda}{l}\sqrt{\cos^2(q_c) - \cos^2(q_n)} \qquad (2)$$

and compared to that determined by high-angle XRD formalism. n represents the order of diffraction, related to the Bragg peak positioned at q_n; L is the modulation period of the multilayer; $q_c \approx 0.4^o$ is the critical angle, below which all radiation is totally reflected; l is the X-ray wavelength.

The low-angle results are very sensitive to changes in the electronic density throughout the sample and less sensitive to the intra-layer disorder. Since the radiation detected results from the contribution of the reflected radiation on the interfaces, the low-angle patterns are above all sensitive to the interface quality and chemical modulation. From the low-angle refinement we can estimate an average rms roughness present at the interfaces (s_{Total}), however limited by the coherence length of the probing radiation:[9]

$$s_{total} = \sqrt{s_{DW}^2 + t_{i-d}^2 + s_c^2 + \left(s_N^{TiAlN} \times d_{TiAlN}\right)^2 + \left(s_N^{Mo} \times d_{Mo}\right)^2} . \qquad (3)$$

In this last equation the refined parameters from the SUPREX program include the width of the inter-diffusion zone at the interface (t_{i-d}), a Debye-Waller (s_{DW}) coefficient that accounts for the waviness of the interfaces and the width of the continuous distribution of the layer thickness (s_c). Surface roughness will be determined by kinetic limitations, a competition between various rates.[13] Moreover, the coherence length of the X-rays at low angles is higher than at high angles, therefore the region that is probed contains several grains, and the waviness of the interfaces is better manifested. Thus the roughness from the refinement of the low-angle XRD spectra should be higher than that from the high-angle refinement.

4. Experimental and calculated results

$Ti_{.4}Al_{.6}N$/Mo PVD-grown multilayer samples

These samples exhibit a dense columnar structure, which was clearly observed through SEM analysis. Fig. 1 illustrates this morphology, for the particular case of a 2.4 μm sample. One apparent effect of the negative potential that was applied to the substrates during the deposition of these multilayers is related to the reduction on the number and size of defects that arise at the surface. The possible mechanism that takes place is related with the void annihilation and a consequent film densification. In Fig. 2 it is obvious how the film surface became cleaner of defects as the bias voltage was increased from 0 to –120V.

An RBS experiment, with respective fit, was performed on a thick and homogeneous (Ti,Al)N coating in order to determine the composition of the individual. From

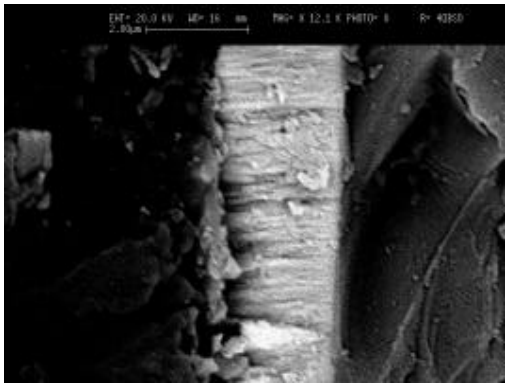

FIG. 1. Cross-section SEM analysis of a $Ti_{.4}Al_{.6}N$/Mo multilayer showing a typical columnar structure.

this result it was obtained that the layers consist of 30 at.% of aluminum, 20 at.% of titanium and about 50 at.%of nitrogen, hence we have $Ti_{0.4}Al_{0.6}N$. According to Y. Setsuhara *et al.*[14], and from the XRD analysis of a thick sample, this stoichiometry evidences a NaCl type structure.

RBS spectra allow only the analysis of the outermost layers of the multilayer. The evolution of the RBS spectra and respective fits for different deposition parameters (taken at an incidence angle of 10º) is illustrated in Fig. 3 for the samples DC1, DC2 and DC3, which have a thickness of about 0.7 μm and a modulation period of approximately 13 nm. These structural data was useful for the determination of the film composition and individual layer thicknesses (in at/cm^2). Sample DC1, prepared without substrate polarization, shows the highest inter-layer average roughness and surface roughness since the individual monolayers cannot be resolved using the RBS technique. Samples DC2 and DC3 were prepared with a substrate polarization of -60 V and -120 V, respectively, having in the former a buffer layer of TiAl with a thickness of ~100 nm and in the latter of a buffer layer Mo with a thickness of ~39 nm. An increase in bias voltage and the consequent increase in the Ar^+ ion energy have the effect of decreasing the multilayer roughness (cf. Fig. 3). Ion bombardment in these samples was relatively high with an ion-to-atom flux ratio (J_i/J_a) at the substrate of the order of 2 for Mo and 12 for $Ti_{.4}Al_{.6}N$. These values were calculated from the ion current density in the substrate holder and from the deposition rate estimated according to the corresponding RBS-calculated thickness in at/cm^2 (cf. Table 2). The decrease in the multilayer roughness is associated with an increase in the residual stress of the multilayer structure. Regarding the individual layer thickness, a reasonable fluctuation is evidenced. This can be explained by the fact that from DC1 to DC2 the bias voltage was increased from 0 to –60 V, hence the heavier ions flux rate and Ar^+ ion energy was enhanced. Additionally, the argon partial pressure for $Ti_{.4}Al_{.6}N$ dropped from 0.35 to 0.3 Pa, which lead to a decrease in the deposition rate for this material. When comparing samples DC1 and DC3 we conclude that the decrease in the thickness was due to re-sputtering effects from a high

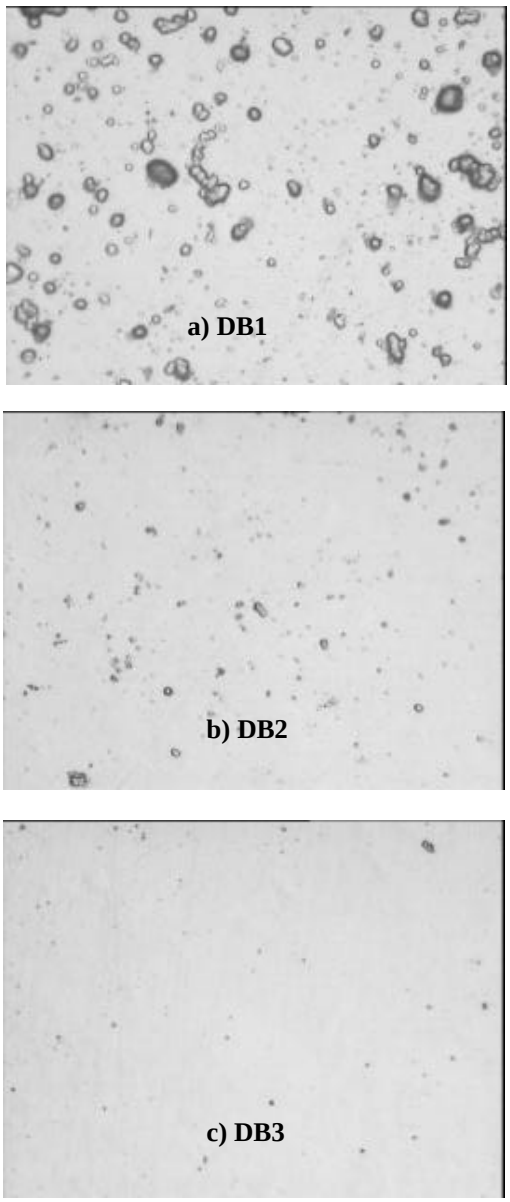

FIG. 2. Morphology of three $Ti_{.4}Al_{.6}N$/Mo samples (a) DB1, (b) DB2 and (c) DB3. As the bias is increased from –60 V to –120 V the surface has fewer defects. The magnification shown is 50x.

voltage present in the substrate holder.

XRD and residual stress

Both low-angle and high-angle scans provided us the modulation periodicity. The Bragg peaks associated with the low-angle patterns are identified up to the 8th order. This allowed the precise determination of the modulation periodicity (L, cf. Table 1), and also positively ensured a good chemical modulation when producing the multilayers. In the high-angle XRD scan of Figure 4 for sample DC2 one can not see a central peak indicating a multilayer preferential growth direction but two main peaks instead. This is due to the large difference in the scattering factors between the multilayer constituents. Since only the first

TABLE 2. Composition of the DC series of $Ti_{.4}Al_{.6}N$/Mo samples obtained by refining the RBS spectra.

Sample	Total thickness (at/cm^2)	Mo (at.%)	Ti (at.%)	Al (at.%)	N (at.%)	Mo thickness (at/cm^2)	$Ti_{.4}Al_{.6}N$ thickness (at/cm^2)
DC1	$4.9x10^{18}$	37	13	19	31	$3.6x10^{16}$	$6.1x10^{16}$
DC2	$4.4x10^{18}$	42	11.5	17.5	29	$3.7x10^{16}$	$5.1x10^{16}$
DC3	$4.2x10^{18}$	36	13	19	32	$3.2x10^{16}$	$5.2x10^{16}$

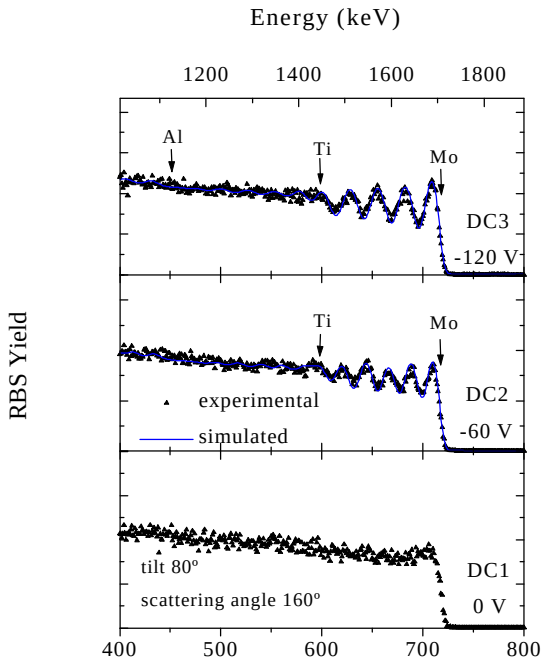

FIG. 3. RBS spectra and RUMP fits corresponding to the DC series of $Ti_{.4}Al_{.6}N$/Mo samples, showing a decrease of the inter-layer roughness with the value of the negative bias potential applied to the substrates during deposition.

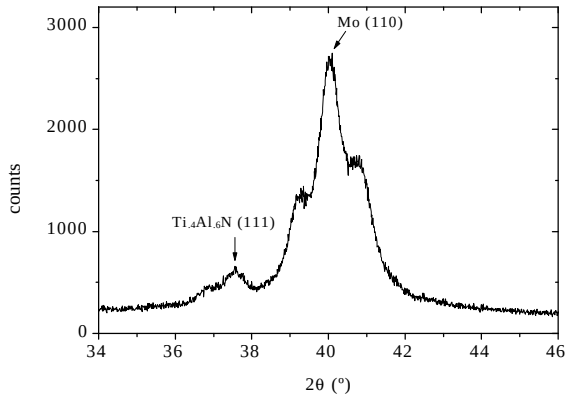

FIG. 4. XRD high-angle scan from sample DC2 consisting of a 50-bilayer $Ti_{.4}Al_{.6}N$/Mo structure with a period of 14.1 nm. Both $Ti_{.4}Al_{.6}N$ (111) and Mo (110) growth directions are viewed.

order satellite peaks were visible in these patterns about the $Ti_{.4}Al_{.6}N$ (111) and Mo (110) direction it is indicative that apossible mechanism that lowers the intensity of these peaks has to be directly related to the roughness of the interfaces. This fact was verified while analyzing the output disorder parameters from the SUPREX XRD refinement program. Due to the fact that the multilayers are polycrystalline other growth directions were visible, namely the $Ti_{.4}Al_{.6}N$ (200) and Mo (200), albeit associated with lower intensities. Both discrete and continuous levels of fluctuation are considerable enhancing the total disorder, leading to roughness rms maximum values of 0.8 nm for bias voltages of –60 V (cf. Table 1). This fact is in agreement with the decrease of the interfacial roughness with increasing bias voltage. Additionally, an improvement in the resolution of the Bragg peaks in the low-angle XRD scans was experimentally noticeable with increasing polarization potential, hence sharper interfaces. From the refinement of the low-angle XRD patterns inter-diffusion distances of the order of 0.4 nm were obtained for all samples. Therefore, an inherent mixing of both species ($Ti_{.4}Al_{.6}N$ and Mo) at the interface is dominant. Additionally, the main peaks in the high-angle scans are very broad indicating in turn a considerable amount of layering defects. The values of L and t_{TiAlN}/t_{Mo} (individual layer thickness ratio) shown in Table 1 were obtained from refining separately the low- and high-angle scans with SUPREX. A good indicator of the reproducibility of these structures is that the modulation period was confirmed to be kept approximately constant at about 14 nm throughout the DB series, fluctuating a little bit in the thinner set (DC series). Fig. 5 shows both refinements for the low- and high-angle patterns associated with sample DB1. In the case of the modulation period, the refined values [cf. Eq. (1)] coincide with the predicted ones using Bragg's equation with a correction for the critical angle [cf. Eq. (2)].

Residual in-plane stress was calculated using Stoney's equation[15] after measuring the curvature of the substrates prior to and after deposition.[16] All samples are under a compressive residual, ranging from approximately –0.2 to –0.5 GPa. A couple of higher values of the order of –1 GPa for particular experimental conditions is related to a high (-120 V) polarization voltage during deposition. From the results in Table 1 we conclude that both the increase of the bias voltage and, to some limit, the argon partial pressure to produce Mo increase the residual stress values. This compressive in-plane stress field is compatible with the out-of-plane tensile (relaxed) stress field detected in the XRD profiles. Both refined perpendicular interplanar

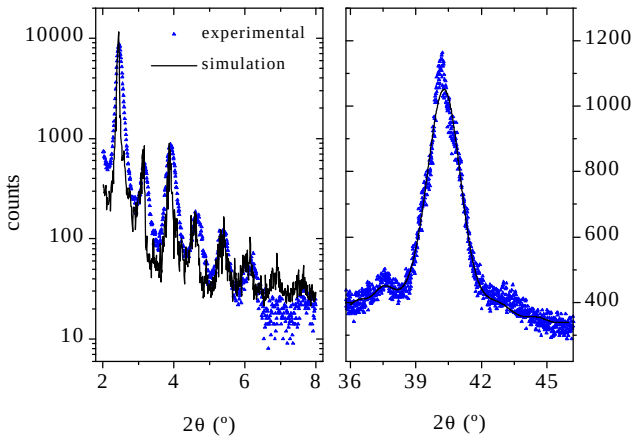

FIG. 5. XRD low- and high-angle spectra and respective SUPREX refinement for sample DB1, consisting of a 200-bilayer $Ti_{.4}Al_{.6}N$/Mo structure with a period of 13.6 nm.

distances (*d*) for $Ti_{.4}Al_{.6}N$ and Mo (2.392 Å and 2.242 Å respectively) are expanded relatively to the bulk ones (2.387 Å and 2.219 Å respectively). Hence, the effect of the bias voltage on these coatings is to increase the state of residual stress as the voltage itself is elevated from 0 to –120V. The lattice mismatch between $Ti_{.4}Al_{.6}N$ and Mo is relatively high (~7%) therefore one shouldn't rule out the possibility of coherency strain effects.

5. Conclusions

We report in this paper the production of $Ti_{.4}Al_{.6}N$/Mo multilayers with a good chemical modulation. In order to study their structural properties RBS, XRD low- and high-angle experiments took place. To gather more information about the structural parameters a computational refinement of the XRD patterns was carried out. An estimation of the surface roughness was possible, however it is limited by the coherency of the X-rays. A higher cumulative roughness, which was not estimated, exists in these coatings since the interfacial disorder increases with film thickness, as proven from RBS experiments. The latter spectroscopy proved to be very useful to determine the film composition. By polarizing the substrates with a negative potential one can control changes in surface morphology, columnar growth, residual stress and inter-layer roughness.

Acknowledgements

The authors gratefully acknowledge the financial support of the "Junta Nacional de Investigação Científica" (JNICT), during the course of this scientific research, under the project referenced as PBICT/P/CTM/1962/95.

References

[1] K.J. Ma, A. Bloyce and T. Bell, Surf. Coat. Technol. **76-77**, 297(1995)
[2] L.A. Donahue, et al., Surf. Coat. Technol. **76-77**, 149 (1995)
[3] D.G. Stearns, J. Appl. Phys. **71**, 4286 (1992)
[4] M.F.da Silva, M.R. da Silva, E.J.Alves, A.A.Melo, J.C.Soares, J.Winand and R.Vianden, *Surface Engineering*, edited by R.Kossowsky and S.Singhal (NATO ASI, Les Arcs, Nijhoff, 1984),74.
[5] L.R. Doolittle, Nucl. Inst. and Meth. **B9**, 344 (1985)
[6] E.E. Fullerton, I.K. Schuller, H. Vanderstraeten and Y. Bruynseraede, Phys. Rev. B, **45**, 9292 (1992)
[7] K. Temst, et al., Appl. Phys. Lett. **67** (23), 3429 (1995)
[8] C.J. Tavares, L. Rebouta, B. Almeida, J. Bessa e Sousa, Surf. Coat. Technol. **100-101**, 65 (1998)
[9] Hans Vanderstraeten, ***PhD. Thesis*** (Katholieke Universiteit Leuven, 1991)
[10] A. Segmüller, A.E. Blakeslee, J. Appl, Cryst. **6**, 19 (1973)
[11] E. Spiller, *Physics, Fabrication and Applications of Multilayered Structures*, edited by P. Dhez and C. Weisbuch (Plenum, New York, 1987) p. 271
[12] Y.S. Gu, W.P. Chai, Z.H. Mai and J.G. Zhao, Phys. Rev. B. **50**, 6119 (1994)
[13] D.E. Savage, N. Schimke, Y.-H. Phang and M.G. Lagally, J. Appl. Phys. **71** (7), 3283 (1992)
[14] Y. Setsuhara et al., Surf. Coat. Technol. **97**, 254 (1997)
[15] G.G. Stoney, Proc. R. Soc. London, Ser. A **82**, 172 (1909)
[16] C.J. Tavares, L. Rebouta, M. Andritschky and S. Ramos, J. Mat. Proc. Technol. **4025**, 1 (1999)